Neutral pion condensation in the chiral SU(3)⊗SU(3) model

Koichi Takahashi
Department of Liberal Arts, Tohoku Gakuin University, Izumi-ku, Sendai 981-3139, Japan
(Received 11 February 2002; published 16 August 2002)

A pure p-wave π^0 condensation in the chiral SU(3)⊗SU(3) model is studied within the relativistic mean-field approximation and its effect on the equation of state is compared with that of a pure s-wave K^- condensation. To this end, three models are considered, which are distinguished from each other in the ways σ, ω, and ρ mesons contribute to the system's energy. We find that, although the details of the result are model dependent, the π^0 condensation forming a standing wave is commonly observed in the intermediate region of density. In particular, in case ω's mass is generated through coupling to σ, π^0 condensation reduces the system's energy significantly. The pure π^0 condensation tends to be taken over by the pure uniform K^- condensation at high densities because of the dominance of the KN sigma term.

DOI: 10.1103/PhysRevC.66.025202 PACS number(s): 12.39.Fe, 26.60.+c

I. INTRODUCTION

The meson condensation in dense matter is expected to affect significantly the physics of a neutron star via both the softening of the equation of state of dense matter and providing a powerful source of weak interaction. In particular, the lightest pseudoscalars, pions, and kaons have so far attracted great attentions of many authors in expectation of incorporating the broken chiral symmetry, an important notion in the phenomenology just above the level of quantum chromodynamics.

An intriguing nonrelativistic analysis of pion condensation within the linear σ model (L σ M) was performed by Dautry and Nyman within the mean-field approximation [1]. They found a variational solution that exhibits a standing wave for chiral fields and a perfect polarization of nucleons. This view was applied later to a relativistic analysis of quark-pion matter [2]. The naive L σ M, however, is known to give unacceptably large compression moduli for the normal nuclear matter [3,4], and has been subject to various modifications to overcome this difficulty [5].

Recently, the L σ M of nucleons and pions was reexamined within a relativistic mean-field approximation for the purpose of finding, at high densities, a stable phase other than the normal one [6]. There, it was confirmed that the chiral fields σ and π^0 form the Dautry-Nyman configuration in symmetric neutron matter at and above a few times normal nuclear matter density n_0. In this state, the axial charge is nonvanishing. In Ref. [6], such a field configuration was referred to as axial wave condensation (AWC). Under the AWC, the Fermi surface is deformed and the nucleons polarize because of the nonvanishing spatial component of the axial current. The nucleons have magnetic moments. This implies that the ground state of high-density matter is likely to be spontaneously magnetized. These results are regarded as a relativistic version of the studies based on the nonrelativistic L σ M [7].

The L σ M generally suffers from the appearance of a tachyon [8]. To avoid this undesirable situation, the pseudoscalar mesons must be treated explicitly as the Nambu-Goldstone modes associated with the breakdown of chiral symmetry. For this purpose, it will be preferable to work within the SU(3)⊗SU(3) nonlinear chiral model. Such an extension of the symmetry group has an additional merit that the remaining particle species as strange hadrons will be systematically incorporated.

The nonlinear chiral SU(3)⊗SU(3) model has long been prevalent as a basic tool in exploring the possibility of kaon condensation (KC) in dense matter since the work of Kaplan and Nelson [9]. There the kaon-nucleon s-wave attraction via the massive strange quark, the major driving force of KC, starts to work at a few times n_0.

In contrast to the familiar KC, the origin of AWC is attributed mainly to the condensation of a light neutral pion with a finite wave vector. Thus, which of the kaon and pion condensations finally governs the equation of state (EOS) becomes an urgent issue in the study of high-density matter based on the chiral SU(3)⊗SU(3) model. In this paper, we calculate the EOS's of neutron star matter in chiral SU(3)⊗SU(3) for K^- condensation and π^0 condensation to see their relative importance.

In the following section, we describe the models based on the Kaplan-Nelson model. In Secs. III and IV, arguments for constructing physical quantities are given for AWC and KC, respectively. In Sec. V, the forms of potentials and the effective nucleon mass are specified. In Sec. VI, the results of numerical calculations are presented. Section VII is devoted to concluding remarks.

II. MODEL

Our model has the same structure as the one adopted by Kaplan and Nelson [9] for the sector of baryons and (pseudo) Nambu-Goldstone bosons,

$$\begin{aligned} L_x=&\frac{f^2}{2}\mathrm{Tr}\partial_\mu U^\dagger \partial^\mu U + c\,\mathrm{Tr}[m_q(U+U^\dagger-2)] \\ &+\mathrm{Tr}\bar{B}(i\partial - m_B)B + i\,\mathrm{Tr}\bar{B}\gamma^\mu[V_\mu,B] \\ &+D\,\mathrm{Tr}\bar{B}\gamma^\mu\gamma_5\{A_\mu,B\}+F\,\mathrm{Tr}\bar{B}\gamma^\mu\gamma_5[A_\mu,B] \\ &+a_1\mathrm{Tr}\bar{B}(\xi m_q\xi+\mathrm{H.c.})B+a_2\mathrm{Tr}\bar{B}B(\xi m_q\xi+\mathrm{H.c.}) \\ &+a_3\mathrm{Tr}\bar{B}B\,\mathrm{Tr}[m_q(U+U^\dagger)], \end{aligned} \tag{2.1}$$

where $U=\xi^2=\exp(\sqrt{2}iM/f)$. V_μ and A_μ are the usual vector and axial vector fields constructed from ξ. The quark mass matrix is given by $m_q=\mathrm{diag}(\bar{m},\bar{m},m_s)$ with $\bar{m}=(m_u+m_d)/2$. The meson and baryon matrices are given by

$$M=\begin{pmatrix} \pi^0/\sqrt{2} & 0 & K^+ \\ 0 & -\pi^0/\sqrt{2} & 0 \\ K^- & 0 & 0 \end{pmatrix}, \quad B=\begin{pmatrix} 0 & 0 & p \\ 0 & 0 & n \\ 0 & 0 & 0 \end{pmatrix}. \tag{2.2}$$

After some algebra, it is possible to obtain a single matrix expression of ξ for the case where π^0 and K simultaneously exist:

$$\xi=\begin{pmatrix} W & 0 & Xe^{i\phi} \\ 0 & Y & 0 \\ Xe^{-i\phi} & 0 & Z \end{pmatrix}, \tag{2.3a}$$

$$W=\cos^2\frac{\varphi}{2}e^{iu\rho\cos^2\varphi/2}+\sin^2\frac{\varphi}{2}e^{-iu\rho\sin^2\varphi/2},$$

$$X=\frac{\sin\varphi}{2}(e^{iu\rho\cos^2\varphi/2}-e^{-iu\rho\sin^2\varphi/2}), \quad Y=e^{-iu\rho\cos\varphi},$$

$$Z=\sin^2\frac{\varphi}{2}e^{iu\rho\cos^2\varphi/2}+\cos^2\frac{\varphi}{2}e^{-iu\rho\sin^2\varphi/2}, \tag{2.3b}$$

with $\phi=\arg(K^+)$, $u=1/\sqrt{2}f$, and ρ and φ being defined by

$$\rho\equiv\sqrt{\pi^{0^2}/2+4K^+K^-}, \quad K^\pm=\beta e^{\pm i\phi},$$

$$\pi^0/\sqrt{2}=\rho\cos\varphi, \quad 2\beta=\rho\sin\varphi. \tag{2.4}$$

However, hereafter we restrict ourselves to the cases either $\pi^0\neq 0$ and $K^\pm=0$ or $\pi^0=0$ and $K^\pm\neq 0$ for clarity of argument. The total Lagrangian is given by

$$L_T=L_\chi+L_{\bar{B}B\sigma}-U_\sigma-U_\omega-U_\rho, \tag{2.5}$$

where the last four terms are, respectively, the contributions from the baryon-σ interaction, and the potentials of σ, ω, and ρ_0 mesons, which play important roles in the relativistic mean-field theory [10]. Their forms will be specified later.

Following the spirit of the relativistic mean-field theory, we push various effects of nuclear forces into the interactions of σ, ω, ρ_0 mesons and nucleons. The relevant model parameters are determined by the nuclear matter data at saturation. On the other hand, for determining the products of the quark masses and the parameters $a_{1,2,3}$ in L_χ, we will use the values of the sigma terms deduced from the experimental data in vacuum. This is the so-called on-shell Σ approximation, which has not yet been satisfactorily validated [11]. This means that the in-medium off-shell extrapolation is somewhat ambiguous and model dependent in the effective Lagrangian formalism [12]. In fact, from the viewpoint of chiral perturbation theory, the f in Eq. (2.1) is expected to be scaled in a density-dependent way [13]. Nevertheless, in this paper, we shall work within the on-shell-Σ approximation since, for the purpose of observing the relative significance of kaon and pion condensations, it will be reasonable to start from a common footing, which may be conveniently provided by choosing the effective Lagrangians appropriately. Many works to calculate the EOS under the KC [14–16] as well as the kaon energy in medium [17] have been done within the effective field theory of this kind. The details of the construction of our model are discussed in the following sections.

III. π^0 CONDENSATION

In order to explore the neutral pion condensation, we set $K^\pm=0$ in the meson matrix M. The positive electric charge carried by protons is neutralized by free electrons. The chiral Lagrangian for the nucleons and the pion is read from L_χ as

$$L_\chi=L_{\pi B}\equiv\frac{1}{2}(\partial_\mu\pi^0)^2-f^2m_\pi^2\sin^2\frac{\pi^0}{\sqrt{2}f}+\bar{\psi}(i\partial-M_{B,\chi})\psi$$
$$-\frac{F+D}{2f}\partial_\mu\pi^0\bar{\psi}\gamma^\mu\gamma_5\tau_3\psi, \tag{3.1}$$

where ψ stands for the SU(2) doublet of a proton and a neutron and τ_3 is the third isospin matrix. For F and D, we use a value $F+D=1.25$. The baryonic mass function $M_{B,\chi}$ is given by

$$M_{B,\chi}=m_B-2a_1\bar{m}-2a_2m_s-2a_3(2\bar{m}+m_s)$$
$$+(2a_1+4a_3)\bar{m}\left(\frac{\pi^0}{f}\right)^2Y(\pi^0), \tag{3.2}$$

where $Y(s)$ is defined by

$$Y(s)\equiv\frac{2f^2}{s^2}\sin^2\frac{s}{\sqrt{2}f}. \tag{3.3}$$

The $L_{BB\sigma}$ in the relativistic mean-field Lagrangian has the form $-M_{\mathrm{RMF}}(\sigma)\bar{\psi}\psi$ and will also contribute to the baryon mass in the absence of π^0,

$$M(\sigma)=M_{B,\chi}|_{\pi_0=0}+M_{\mathrm{RMF}}(\sigma). \tag{3.4}$$

The effective baryon mass under the π^0 condensation is then expressed as

$$M_B=M(\sigma)+(2a_1+4a_3)\bar{m}\left(\frac{\pi^0}{f}\right)^2Y(\pi^0). \tag{3.5}$$

We first recall that, in L σ M, the pseudoscalar coupling $\pi^0 i\bar{\psi}\gamma_5\tau_3\psi$ [pseudoscalar representation (PSR)] was chiral-rotated away and transmuted to an axial vector coupling $\frac{1}{2}\partial_\mu\Omega\bar{\psi}\gamma^\mu\gamma_5\tau_3\psi$ [axial vector representation (AVR)] by $\psi_{\mathrm{PS}}=\exp(-i\gamma_5\tau_3\Omega/2)\psi_{\mathrm{AV}}$ with obvious meanings of subscripts [1,6]. Here, a chiral angle Ω has been defined by $\pi^0/\sigma=\tan\Omega$. Then, $\Omega=kz$ was substituted into the Lagrangian and the equation of motion for ψ_{AV} was solved. Using the solutions found in Refs. [1,18], we see that the corresponding eigenfunctions u_{AV} render the scalar density $\rho_{\mathrm{AV}}\equiv\bar{u}_{\mathrm{AV}}u_{\mathrm{AV}}$ finite and the pseudoscalar density $\rho_{5,\mathrm{AV}}\equiv i\bar{u}_{\mathrm{AV}}\gamma_5\tau_3u_{\mathrm{AV}}$ to vanish. This means that, for PSR,

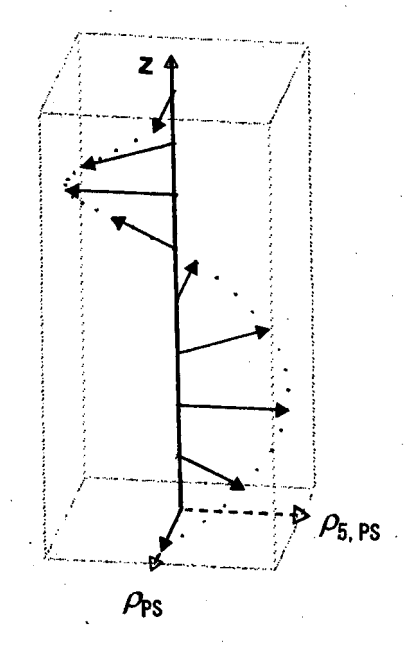

FIG. 1. Schematic view of a helix structure of $(\langle\bar{\psi}\psi\rangle,\langle i\bar{\psi}\gamma_5\tau_3\psi\rangle)$ for PSR with $\tau_3=1$ in AWC.

$$\rho_{\mathrm{PS}}\equiv\bar{u}_{\mathrm{PS}}u_{\mathrm{PS}}=\rho_{\mathrm{AV}}\cos kz,$$

$$\rho_{5,\mathrm{PS}}\equiv i\bar{u}_{\mathrm{PS}}\gamma_5\tau_3 u_{\mathrm{PS}}=-\rho_{\mathrm{AV}}\sin kz. \tag{3.6}$$

Thus, a two-dimensional vector $(\rho_{\mathrm{PS}},\rho_{5,\mathrm{PS}})$ rotates along the z axis as is depicted in Fig. 1. The AWC is the chiral field configuration that brings about the effect of this kind on the fermion sector.

In the nonlinear model, the chiral angles represent the Goldstone fields. Then, the classical pion field that will give rise to an effect analogous to the AWC is given simply by a linear function of spatial coordinates,

$$\pi^0=fkz. \tag{3.7}$$

Here k is a constant. The equation of motion of nucleon in the AVR reads

$$(i\partial-\tfrac{1}{2}\tilde{k}\gamma^3\gamma_5\tau_3-M_B)\psi=0, \tag{3.8}$$

where $\tilde{k}\equiv(F+D)k$. Since M_B given by Eq. (3.5) is spatially oscillating, solving Eq. (3.8) is not an easy task. Instead of dealing with Eq. (3.8) as it is, we replace M_B by its spatial average,

$$\bar{M}_B\equiv V^{-1}\int M_B(\mathbf{x})d\mathbf{x}=M(\sigma)+\Delta M,$$

$$\Delta M=-\Sigma_{\pi N}=(2a_1+4a_3)\bar{m}, \tag{3.9}$$

where $\Sigma_{\pi N}$ is the πN sigma term in vacuum: $\Sigma_{\pi N}=\bar{m}\partial M_B|_{\pi_0=0}/\partial\bar{m}$. This procedure is equivalent to assuming, on taking the expectation value of the Hamiltonian, the Fermi sea being filled with nucleons in single particle states of plane-wave forms. This may not be a bad approximation when $\bar{m}$ is regarded small enough as compared to the characteristic energy scale appearing in high-density regions we are interested in [18]. The value of $\Sigma_{\pi N}$ estimated from the πN scatterings lies in a wide range [19]. Inputting values of a_1's and $\bar{m}\sim m_s/30$ given in the literature [15,20], we have $\Sigma_{\pi N}\approx(2.67+4.220)/30\ \mathrm{MeV}\approx(34\pm5)\ \mathrm{MeV}$. We will calculate EOS of the AWC phase for $\Sigma_{\pi N}=30$ MeV. This value will turn out not to necessarily be a negligible one when we later compare binding energies per baryon for various models. A notable feature is that $\Delta M<0$, i.e., the AWC is expected to provide an s-wave attraction in a sense of average, as long as the up and down quarks are massive.

The energy eigenvalue of Eq. (3.8) for a momentum $\mathbf{q}$ is given by [1,6,18]

$$\omega_{\pm}(\mathbf{q})=\left[q_1^2+q_2^2+\left(\sqrt{q_3^2+\bar{M}_B^2}\pm\frac{1}{2}\tilde{k}\right)^2\right]^{1/2}, \tag{3.10}$$

with the double sign corresponding to two spin polarizations. There exists an energy gap $\tilde{k}$ between the higher and lower branches. When $\tilde{k}$ is sufficiently large, the Fermi sea of nucleons is formed by filling the levels of lower branch ω_-. The energy density of the nucleon i ($i=n$ or p) thus obtained is

$$\varepsilon_i=\frac{\gamma_s}{2\pi^2}\left\{\left(\frac{E_F^{(i)}}{4}-\frac{5\tilde{k}}{24}\right)q_F^{(i)3}+\frac{\bar{M}_B^2-\tilde{k}^2}{8}\left[\left(E_F^{(i)}+\frac{\tilde{k}}{2}\right)q_F^{(i)}-\bar{M}_B^2\ln\frac{E_F^{(i)}+q_F^{(i)}+\frac{1}{2}\tilde{k}}{\bar{M}_B}\right]\right\}. \tag{3.11}$$

where $\gamma_s=1$ is the factor of spin degeneracy, $E_F^{(i)}$ is the Fermi energy of the nucleon i, and $q_F^{(i)}$, the longer half-radius of the deformed Fermi surface, is given by

$$q_F^{(i)}=\sqrt{\left(E_F^{(i)}+\frac{1}{2}\tilde{k}\right)^2-\bar{M}_B^2}. \tag{3.12}$$

The $E_F^{(i)}$ and the particle number density n_i are related by

$$n_i=\frac{\gamma_s}{4\pi^2}\left[\frac{q_F^{(i)}}{3}\left(2E_F^{(i)2}-2\bar{M}_B^2-\frac{\tilde{k}^2}{4}+\frac{\tilde{k}}{2}E_F^{(i)}\right)+\frac{\tilde{k}}{2}E_F^{(i)2}\ln\frac{E_F^{(i)}+q_F^{(i)}+\frac{1}{2}\tilde{k}}{\bar{M}_B}\right]. \tag{3.13}$$

The total baryon number density is given by $n=n_n+n_p$. In case the Fermi energy exceeds $\bar{M}_B+\tilde{k}/2$, the higher branch must also be taken into account. When $\bar{M}_B>\tilde{k}/2$ (this is a case we encounter in numerical calculations given below), the physical quantities for the higher branch are obtained by a replacement $k\to-k$ in the expressions (3.11)–(3.13). The average energy density for $L_{\pi B}$ thus reads

$$\varepsilon_{\pi B}=\varepsilon_n+\varepsilon_p+\tfrac{1}{2}f^2(k^2+m_\pi^2). \tag{3.14}$$

where $\sin^2(\pi^0/\sqrt{2}f)$ in Eq. (3.1) has been replaced by $\frac{1}{2}$.

Obviously, the PSR of Eq. (3.1) is obtained by $\psi_{\rm AV}=e^{-i(F+D)\pi^0\gamma_5\tau_3/2f}\psi_{\rm PS}$. The chiral angle corresponding to this transformation is given by $-\tilde{k}z$, which yields $(\rho_{\rm PS},\rho_{5,\rm PS})\propto(\cos\tilde{k}z,\sin\tilde{k}z)$, i.e., a helix structure shown in Fig. 1. The configuration of this kind is analogous to the atomic spin configuration called spin-density wave in solid state physics [21]. This analogy seems to become more pertinent if we note that $S_1=\frac{1}{2}\int d\mathbf{x}\,\bar{\psi}\psi$, $S_2=\frac{1}{2}\int d\mathbf{x}i\,\bar{\psi}\gamma_5\tau_3\psi$, and $S_3=\frac{1}{2}Q_{5,nL}=\frac{1}{2}\int d\mathbf{x}\,j^0_{5,nL}$ are "chiral spin" operators: $[S_i,S_j]=i\varepsilon_{tjk}S_k$ for static meson fields. If the symmetry were exact, S_3 would be conserved and could be used as a quantum number to characterize the system. Unfortunately, this is not an exact symmetry for the situation under consideration. Nevertheless, the quantities associated with these operators are expected to be useful in characterizing the AWC phase of high-density nuclear matter.

We here give a brief remark on charged pion condensation. Because of an advantage in fulfilling the charge neutrality condition, the π^- condensation has been of a wide interest in the physics of neutron star matter. Within the LσM, Dautry and Nyman have made an estimation of the effect of the π^- condensation to the system's energy and compared it with that of the $\sigma\pi^0$ condensate (i.e., AWC) under a familiar assumption [1],

$$\pi_1\pm i\pi_2=re^{\pm i\mathbf{q}\cdot\mathbf{z}}\sin\theta,$$

$$\sigma\pm i\pi_3=re^{\pm i\mathbf{k}\cdot\mathbf{x}}\cos\theta. \tag{3.15}$$

They found that the contribution of π^- is small as compared to the AWC of σ and π_3. Using their solution [Eq. (3.2) in Ref. [1]] for the nucleon wave function, the chiral spin vector for the configuration (3.15) is given by

$$\rho_{\rm PS}=\rho_{\rm AV}\cos\mathbf{k}\cdot\mathbf{x}-\rho_{5,\rm AV}\sin\mathbf{k}\cdot\mathbf{x},$$

$$\rho_{5,\rm PS}=\rho_{\rm AV}\sin\mathbf{k}\cdot\mathbf{x}+\rho_{5,\rm AV}\cos\mathbf{k}\cdot\mathbf{x}, \tag{3.16}$$

where $\rho_{\rm AV}$ and $\rho_{5,\rm AV}$ are independent of the spatial coordinate. A pure π^- condensation may imply $\mathbf{k}=\mathbf{0}$ and thus no spatial dependence in $(\rho_{\rm PS},\rho_{5,\rm PS})$. In our terminology, the chiral spin density wave does not form for a pure π^- condensation. This feature of pion condensation will remain essentially unaltered in the nonlinear model, too. (One might think of a configuration such as $\pi_1\pm i\pi_2=f\mathbf{k}\cdot\mathbf{x}e^{\mp i\mu_\pi t}$. However, its kinetic energy is divergent for $\mu_\pi\neq0$.) Although the effect of the charged pion has to be eventually clarified, we here expect that the assumption of the dominance of AWC is not a bad approximation as long as the pion condensation in the chiral model is concerned.

IV. K^- CONDENSATION

The kaon condensed phase in the Kaplan-Nelson model [9] has been studied intensively by many authors for various situations including neutral kaon and hyperons. In the present study, we consider a pure uniform K^- condensation for the sake of simplicity and set $\pi^0=0$ in Eq. (2.2).

The exact electric U(1) invariance of the model implies that the expectation value of charged field with respect to the ground state with a fixed baryon number should vanish unless the corresponding chemical potential vanishes [22]. Therefore, for a uniform condensation of a charged kaon, we assume

$$\langle K^-\rangle=0,\quad \langle K^+K^-\rangle=s^2\neq0, \tag{4.1}$$

while, for the operator,

$$K^-=\frac{1}{\sqrt{2\omega V}}(e^{-i\mu t}c+e^{i\bar{\mu}t}\bar{c}^\dagger). \tag{4.2}$$

with c and $\bar{c}$ the annihilation operators of K^- and K^+ with zero momentum, respectively, ω is a parameter with a dimension of mass and V is the system's volume. Then, the canonical quantization

$$[K^-,\Pi_K]=i,\quad \Pi_K=V\delta L_\chi/\delta\dot{K}^-, \tag{4.3}$$

and the construction of the ground state Φ having a three-body correlation $\langle\bar{n}pK^-\rangle$ follow [23]. In this method, the parameter μ appearing in Eq. (4.2) has a meaning of the chemical potential of K^-. This can be seen by evaluating the two-point Green's function $G_K(t)=\langle\Phi|TK^+(t)K^-(0)|\Phi\rangle$ for the kaon field and observing that the Fourier transform of $G_K(t)$ has a pole at μ. Thus creating one K^- in the medium costs the energy of μ. Similarly, $\bar{\mu}$ is the chemical potential of K^+. The canonical quantization condition and the normalization condition of the kaon field operator uniquely determine μ and $\bar{\mu}$ as functions of the baryon number density n, the kaon concentration y and s defined by Eq. (4.1),

$$\omega=\frac{ny}{2s^2}, \tag{4.4a}$$

$$\mu=\frac{ny}{f^2\sin^2\dfrac{\sqrt{2}s}{f}}\left(1-(1+y)\sin^2\frac{s}{\sqrt{2}f}\right), \tag{4.4b}$$

$$\bar{\mu}=2\omega-\mu. \tag{4.4c}$$

Now we give the Lagrangian for K^- and nucleons,

$$L_\chi=L_{\rm KB}\equiv\dot{K}^+\dot{K}^-Y(2s)-m_K^2s^2Y(s)+\bar{\psi}(i\partial-M_B)\psi + \frac{i}{8f^2}(K^+\dot{K}^--\text{H.c.})Y(s)\bar{\psi}(3+\tau_3)\psi, \tag{4.5}$$

where the function $Y(s)$ has been defined by Eq. (3.3). The effective baryon mass M_B is now given by

$$M_B=M(\sigma)+\left(\frac{a_1}{2}(1+\tau_3)+a_2+2a_3\right)M_s\left(\frac{s}{f}\right)^2Y(s). \tag{4.6}$$

TABLE I. Parameters of model I and II.

	r_m	K (MeV)	c_ω	c_p	c_0 (fm^{-2})	c_1	c_2	c_3	D	α_0	α_1	α_2
I	0.85	300	45.3	28	0	33.8	−72.8	1.52	0	1	0	0
II	0.74	240	86.6	25.4	−11.8	−42	−241	−413	−83	0.45	1.1	−0.548

M_B is dependent on τ_3. However, because of the relative smallness of a_1, we simply drop τ_3 in Eq. (4.6) and express M_B in terms of the KN sigma term in vacuum: $\Sigma_{\rm KN} = -(a_1/2 + a_2 + 2a_3)m_s$. We will perform numerical calculations for $\Sigma_{\rm KN} = 300$ and 400 MeV. The electric charge of protons is supposed to be neutralized by K^- and electrons.

Our approach may form a contrast to the conventional mean-field approximation that assumes a finite classical K field with a single oscillation mode

$$\langle K^- \rangle = e^{-i\mu_c t} K_c, \tag{4.7}$$

where μ_c is the charge chemical potential. For pure K^- condensation, this happens to result in a classical Lagrangian identical in appearance to the one derived by our method, provided that K_c is identified with s defined by Eq. (4.1). However, the μ_c, treated as a variational parameter there, can be determined by a numerical method under the charge neutrality condition.

V. CONTRIBUTIONS OF SCALAR AND VECTOR MESONS

The model involves a number of free parameters that are not determined by a symmetry requirement only. They are constrained by observational data as the free hadron masses, in particular, the free nucleon mass $M_0 = 939$ MeV, the πN sigma term $\Sigma_{\pi N} \sim 30$ MeV, the KN sigma term $\Sigma_{\rm KN} \sim 300$–400 MeV, and such nuclear matter data at saturation as the effective nucleon mass ratio $r_m \equiv M^*/M_0 = 0.6$–0.8, the binding energy per baryon $E_b = 16$ MeV, the symmetry energy $a_{\rm sym} = 32$ MeV, the incompressibility $K = 150$–350 MeV, the saturation density $n_0 = 0.16$–0.17 fm^{-3}. However, there still is room allowing some variants in the details of model structure and the global property of EOS. Those variants are specified by distinct functional forms of the scalar potentials, the contributions of vector mesons and the nucleon mass function.

We first consider a model exploited by Sahu and Onishi [24] in constructing the EOS of normal neutron star matter within the L σ M. There, the σ potential and the nucleon mass without pseudoscalar condensation, $M(\sigma)$, are given by

$$U_{\sigma,\rm I}(\sigma) = \frac{c_0}{2}(\sigma-\sigma_0)^2 + \frac{c_1}{4}(\sigma^2-\sigma_0^2)^2 + \frac{c_2}{6\sigma_0^2}(\sigma^2-\sigma_0^2)^3 + \frac{c_3}{8\sigma_0^4}(\sigma^2-\sigma_0^2)^4 - D\sigma_0\left(\tfrac{2}{3}\sigma_0^3 - \sigma_0^2\sigma + \tfrac{1}{3}\sigma^3\right), \tag{5.1}$$

$$M_{\rm I}(\sigma) = g_\sigma \sigma \left[\alpha_0 + \alpha_1 \left(\frac{\sigma}{\sigma_0}\right)^2 + \alpha_2 \left(\frac{\sigma}{\sigma_0}\right)^4 \right], \tag{5.2}$$

with $c_0 = D = 0$, $\alpha_0 = 1$, $\alpha_1 = \alpha_2 = 0$. The vacuum is given by $\sigma = \sigma_0$. In vacuum, the reflection symmetry under $\sigma \to -\sigma$, $\psi \to \gamma_5 \psi$ is broken spontaneously and the nucleon acquires a mass $M_1(\sigma_0) = M_0$. Together with the condition $\sigma_0 = f = 93$ MeV met in the LσM, this yields $g_\sigma = 10.1$. The nucleon effective mass and the incompressibility are taken as $r_m = 0.85$ and $K = 300$ MeV. The ω and the ρ^0 potentials are chosen as

$$U_{\omega,I}(\sigma) = \frac{1}{2} c_{\omega,I} \left(\frac{n}{g_\sigma \sigma}\right)^2, \quad U_{\rho,I} = \frac{1}{2} c_{\rho,I} \left(\frac{n}{M_0}\right)^2 (1-2x)^2, \tag{5.3}$$

where x is the proton fraction. The Boguta scheme [25] is applied to ω meson, whose mass is determined through the coupling to σ field. On the other hand, the ρ^0's mass is a fixed parameter. Treating the ρ^0 contribution in such a manner yields a softer EOS of neutron rich matter.

The M, U_σ, and U_ω in the second model have exactly the same functional forms as given above, but with different values of parameters. The form of U_ρ is changed as

$$U_{\rho,\rm II} = \frac{1}{2} c_{\rho,\rm II} \left(\frac{n}{g_\sigma \sigma}\right)^2 (1-2x)^2. \tag{5.4}$$

That is, the Boguta scheme is applied to both of the ω and the ρ^0 mesons. With this extension of the parameter space, we hope to explore a wider region of the effective nucleon mass and the incompressibility at saturation.

The third model is given by

$$U_{\sigma,\rm III}(\sigma) = \frac{\frac{1}{2} f m_\sigma^2 \sigma^2 + \frac{1}{2} B_\sigma \sigma^3 + \frac{1}{2} C_\sigma \sigma^4}{1 + \frac{1}{2} A_\sigma \sigma^2}, \tag{5.5}$$

$$M_{\rm III}(\sigma) = M_0 - g_\sigma \sigma, \tag{5.6}$$

$$U_{\omega,\rm III} = \frac{1}{2} c_{\omega,\rm III} \left(\frac{n}{M_0}\right)^2, \quad U_{\rho,\rm III} = \frac{1}{2} c_{\rho,\rm III} \left(\frac{n}{M_0}\right)^2 (1-2x)^2. \tag{5.7}$$

In this model, the vacuum is given by $\sigma = 0$. This set of potentials and mass function was adopted by Fujii *et al.* [16] in the analysis of KC in a neutron star matter with a low incompressibility. The vector meson masses in their model are fixed. For other parameters, see Ref. [16]. In our analysis, we adopt the parameter set PM2 in Ref. [16] which yields EOS with intermediate stiffness. The KC has been found to set in at $n \approx 0.5$ fm^{-3}, and the binding energy per baryon

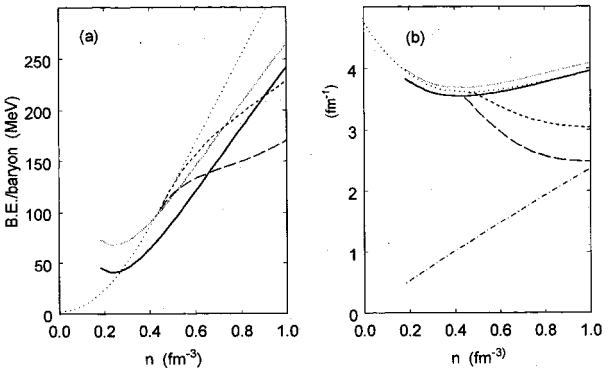

FIG. 2. (a) Energy per baryon for model I. Dotted curve, normal phase; short dashed curve, KC with $\Sigma_{\mathrm{KN}}=300$ MeV; long dashed curve, KC with $\Sigma_{\mathrm{KN}}=400$ MeV; black solid curve, AWC; gray solid curve, fictitious AWC with $\Sigma_{\pi N}=0$. (b) Effective nucleon mass and k for model I. Meanings of dotted, short dashed, long dashed, black solid, and gray solid curves are same as in (a). Dash-dotted curve, k in AWC.

under the KC is reduced from the normal phase by about 30 MeV at $n\approx 0.8$ fm^{-3}. The values of parameters used in models I, II, and III are given in Table I.

VI. NUMERICAL CALCULATIONS

The binding energies per baryon for three models over the density region $0<n<1$ fm^{-3} are shown in Figs. 2–4. In model I, along with the increase in density, the phase of minimum energy changes from the normal phase to the one with AWC, which is finally taken over by KC as is shown in Fig. 2(a). The density ranges of the AWC phase are 0.63 and 0.39 fm^{-3} for $\Sigma_{\mathrm{KN}}=300$ and 400 MeV, respectively. In order to observe the effect of $\Delta M(=-\Sigma_{\pi N})$ in Eq. (3.9), a calculation of EOS for $\Delta M=0$ is also done and the result is shown by a gray curve in the same figure. The value of E_b gets about 25 MeV larger and the region of AWC phase shrinks to 0.28 and 0.09 fm^{-3} for $\Sigma_{\mathrm{KN}}=300$ and 400 MeV, respectively. This means that the finiteness of the πN-sigma term provides one of the key mechanisms in reducing system's energy by the AWC. The effective mass of nucleons increases above $n=0.4$ fm^{-3} for the normal and the AWC phases, while, for the KC phase, continues to decrease down to 3 fm$^{-1}\approx 590$ MeV for $\Sigma_{\mathrm{KN}}=300$ MeV and 2.5 fm$^{-1}\approx 490$ MeV for $\Sigma_{\mathrm{KN}}=400$ MeV, respectively. The decrease of the effective mass is larger for a larger KN-sigma term. The wave vector k in the AWC phase increases almost linearly with the density. The interplay of the finite $\Sigma_{\pi N}$ and the finite k in AWC gives rise to an appreciable reduction of energy in the intermediate density range.

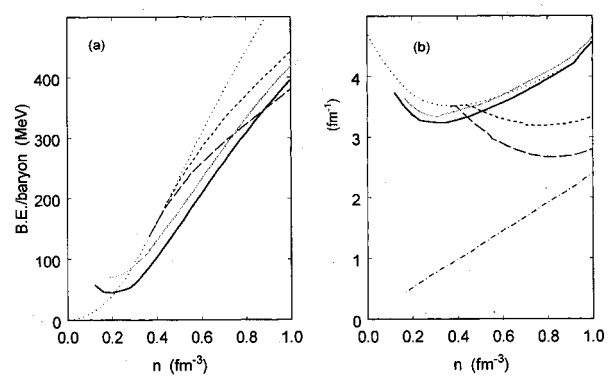

FIG. 3. (a) Energy per baryon for model II. Meanings of curves are same as in Fig. 2. (b) Effective nucleon mass and k for model II. Meanings of curves are same as in Fig. 2.

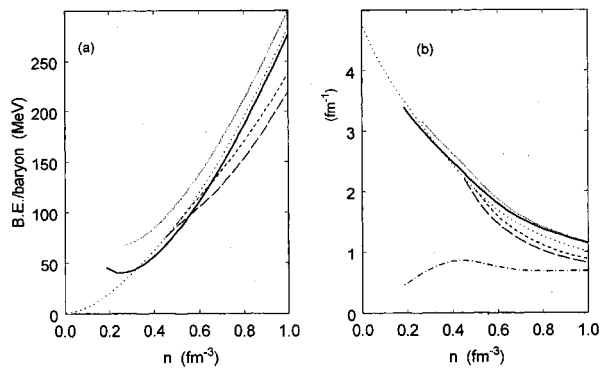

FIG. 4. (a) Energy per baryon for model III. Meanings of curves are same as in Fig. 2. (b) Effective nucleon mass and k for model III. Meanings of curves are same as in Fig. 2.

Model II with $r_m=0.74$ and $K=240$ MeV has stiffer EOS's for all three phases than model I, as is shown in Fig. 3(a). For the case $\Sigma_{\mathrm{KN}}=400$ MeV, the region where the AWC is favored is $0.21<n<0.9$ fm^{-3}, above which the KC takes over. For $\Sigma_{\mathrm{KN}}=300$ MeV, the KC phase is not realized in $n<1$ fm^{-3}. The wider density range for AWC phase is obviously attributed to the large effective nucleon mass M^* shown in Fig. 3(b): the dispersion relation (3.9) implies that, for a sufficiently large effective mass, developing k and reducing the energy levels of the lower branch can reduce the energy of Fermi sea as compared with forming the sea by nucleons with the normal dispersion relation (i.e., $k=0$).

The EOS's for model III with $r_m=0.75$ and $K=200$ MeV are shown in Fig. 4(a). In the AWC phase of this model, the Fermi sea accommodates not only the lower branch, but also the higher branch of neutrons. Even if this is taken into consideration, the AWC costs a large E_b and its region is as narrow as 0.33 and 0.24 fm^{-3} for $\Sigma_{\mathrm{KN}}=300$ and 400 MeV, respectively. For $\Delta M=0$, AWC never takes place. This feature of EOS again has a relevance to the behaviors of effective nucleon mass M^*: it rapidly decreases to as small a value as 200 MeV around $n=1$ fm^{-3} as is shown in Fig. 4(b). When M^* is small enough, Eq. (3.10) implies that filling the lower level in the AWC phase costs almost the same energy as the normal Fermi sea with $\gamma_s=2$ and $k=0$. Therefore, the AWC does not make so much effects on the KC as it does in models I and II.

The EOS's under KC for model III calculated by the conventional mean-field approximation have been reported in Ref. [16]. We note that they almost coincide with the ones obtained by our method.

VII. CONCLUDING REMARKS

We calculated, within the relativistic mean-field approximation, the EOS's of neutron star matter in the nonlinear chiral $SU(3)\otimes SU(3)$ theory of nucleons and mesons. Three phases are considered. The first is the normal phase of nucleons and leptons, which is realized at lower densities. The second one is the phase with charged kaons in a uniform condensation, which has customarily been considered to be realized at higher densities. The last one is a phase that consists of neutral pions in AWC and polarized nucleons. In order to observe the inter-relation among these phases, three different models were adopted as examples, each of which is characterized by the forms of potentials, the values of the incompressibility, the effective nucleon mass at saturation, and so on. Each model calculation was performed for two values of the KN sigma term: $\Sigma_{\mathrm{KN}}=300$ and 400 MeV. We found that, for all of those models, the matter undergoes the first order phase transition from the normal to the AWC phase at $0.2-0.3\,\mathrm{fm}^{-3}$. Models with larger effective nucleon mass tend to have a wider density region of the AWC. The role of the πN-sigma term in AWC is crucial: if the masses of up and down quarks, and therefore $\Sigma_{\pi N}$, are assumed to vanish, then the region of AWC drastically diminishes. On the contrary, if values larger than 30 MeV were used for $\Sigma_{\pi N}$, the AWC phase would possibly be predominant over other phases in the density region relevant to interior of neutron stars.

Some comments are in order. One can regard the chiral symmetry to be not a necessary but a sufficient condition for the AWC to take place. The key mechanism is a generation of the axial vector current, whose time component is the chiral charge and the spatial component is the spin. In fact, some authors, stressing on the importance of axial vector coupling between the baryon and pion, have shown the possibility of nucleon polarization in dense matter in the absence of chiral symmetry [26].

Because of the KN-sigma term in Eq. (4.6), it may be another possibility that kaons (presumably neutral) in a standing wave condensation as well play a role to reduce the energy of AWC phase further. The exploration of the simultaneous condensation of pions and kaons (p-wave $\overline{K}^0$ in addition to the s-wave K^-), together with a quantitative evaluation of the effect of charged pion condensation, thus becomes an intriguing issue in the context of our approach to the study of dense matter.

[1] F. Dautry and E. M. Nyman, Nucl. Phys. **A319**, 323 (1979).
[2] M. Kutschera, W. Broniowski, and A. Kotlorz, Nucl. Phys. **A516**, 566 (1990).
[3] A. K. Kerman and L. D. Miller, LBL-3675, 1974, p. 73.
[4] I. Mishustin, J. Bondorf, and M. Rho, Nucl. Phys. **A555**, 215 (1993).
[5] E. K. Heide, S. Rudaz, and P. J. Ellis, Phys. Lett. B **293**, 259 (1992); R. J. Furnstahl, B. D. Serot, and H.-B. Tang, Nucl. Phys. **A598**, 539 (1996).
[6] K. Takahashi and T. Tatsumi, Phys. Rev. C **63**, 015205 (2000).
[7] G. Baym, D. Campbell, R. Dashen, and J. Manassah, Phys. Lett. **58B**, 304 (1975); C. K. Au, *ibid.* **61B**, 300 (1976).
[8] W. Bentz, L. G. Liu, and A. Arima, Ann. Phys. **188**, 61 (1988); K. Wehrberger, R. Wittman, and B. Serot, Phys. Rev. C **42**, 2680 (1990).
[9] D. B. Kaplan and A. E. Nelson, Phys. Lett. B **175**, 57 (1986); **179**, 40(E) (1986).
[10] S. A. Chin and J. D. Walecka, Phys. Lett. **52B**, 24 (1974); M. Prakash, P. J. Ellis, E. K. Heide, and S. Rudaz, Nucl. Phys. **A575**, 583 (1994), and references cited therein.
[11] H. Yabu, S. Nakamura, and K. Kubodera, Phys. Lett. B **317**, 269 (1993).
[12] J. Delorme, M. Ericson, and T. E. O. Ericson, Phys. Lett. B **291**, 379 (1992).
[13] G. E. Brown and M. Rho, Phys. Rev. Lett. **66**, 2720 (1991); C.-H. Lee, Phys. Rep. **275**, 255 (1996).
[14] B. W. Lynn, A. E. Nelson, and N. Tetradis, Nucl. Phys. **B345**, 186 (1990).
[15] H. M. Prakash, I. Bombaci, M. Prakash, P. J. Ellis, J. M. Lattimer, and R. Knorren, Phys. Rep. **280**, 1 (1997).
[16] H. Fujii, T. Maruyama, T. Muto, and T. Tatsumi, Nucl. Phys. **A597**, 645 (1996).
[17] J. Schaffner, A. Gal, I. N. Mishustin, H. Stocker, and W. Greiner, Phys. Lett. B **334**, 268 (1994); P. J. Ellis, R. Knorren, and M. Prakash, *ibid.* **349**, 11 (1995); G. Mao, P. Papazoglou, S. Hofmann, S. Schramm, H. Stocker, and W. Greiner, Phys. Rev. C **59**, 3381 (1999).
[18] K. Takahashi and T. Tatsumi, Prog. Theor. Phys. **105**, 437 (2001).
[19] E. Reya, Rev. Mod. Phys. **46**, 545 (1974).
[20] H. Georgi, *Weak Interactions and Modern Particle Theory* (Benjamin/Cummings, California, 1984).
[21] A. W. Overhauser, Phys. Rev. Lett. **4**, 462 (1960); Phys. Rev. **128**, 1437 (1962).
[22] K. Takahashi, Phys. Rev. C **58**, 1341 (1998).
[23] K. Takahashi, Prog. Theor. Phys. **98**, 953 (1997).
[24] P. K. Sahu and A. Ohnishi, Prog. Theor. Phys. **104**, 1163 (2000).
[25] J. Boguta, Phys. Lett. **120B**, 34 (1983).
[26] B. Banerjee, N. K. Glendenning, and M. Gyulassy, Nucl. Phys. **A361**, 326 (1981); S. Marcos and R. Niembro, Phys. Lett. B **271**, 277 (1991).